COLLAPSE ANALYSIS OF STRUCTURES WITH MATERIAL AND GEOMETRIC NONLINEARITY BY THE FINITE ELEMENT METHOD

Carlos Melchor

Raul Rosas e Silva

raul@puc-rio.br

Department of Civil Engineering – PUC-Rio

Rua Marques de Sao Vicente 225, CEP 22451-900 Rio de Janeiro, RJ, Brazil

Deane Roehl

droehl@puc-rio.br

Department of Civil Engineering – PUC-Rio

Rua Marques de Sao Vicente 225, CEP 22451-900 Rio de Janeiro, RJ, Brazil

Abstract. *This work presents the critical load estimation of a circular shallow arch through a finite element analysis (FEA). Three kinds of techniques for collapse load estimation using FEA were employed: linear buckling, nonlinear buckling and full nonlinear analysis. For linear buckling analysis an eigenvalue linear analysis was done to estimate the critical load of ideal linear elastic structure. For nonlinear buckling analysis, eigenvalue analysis was performed for critical load in an incremental manner based on the updated stiffness matrices in order to consider material and geometrical nonlinearities. For full nonlinear analysis, the entire equilibrium path is followed up to and possibly beyond the critical load level, updating the stiffness matrix through all the incremental-iterative process. A Finite Element (FE) computational program has been developed using plane stress isoparametric bidimensional elements to perform the three previous mentioned analysis techniques. The results of the FEA show the influence of geometric and material nonlinearity in the critical load estimation. Comments are presented on the errors obtained with linear buckling analysis in determination of critical loads and buckling modes.*

Keywords: *Finite elements, Buckling, Collapse analysis, Critical load, Nonlinear analysis*

1 INTRODUCTION

Nowadays, an understanding of structural behavior during partial or complete collapse is sometimes needed to assess the overall integrity of the structural design under extreme loading scenarios. To perform this, most commercial FE codes employ two categories of collapse or buckling analyses: eigenvalue analysis and full nonlinear analysis.

The eigenvalue analysis identifies the buckling or collapse state of a structure once the structure's stiffness matrix becomes a singular matrix. An eigenvalue analysis, which is formulated assuming a linear elastic behavior to obtain the critical load, is known as linear buckling analysis. This approach is generally used to estimate critical loads of ideal structures in which the change in geometry and stresses prior to buckling is disregarded. On the other hand, the eigenvalue analysis can also be performed in a nonlinear problem updating the incremental stiffness matrices. In this analysis an eigenvalue problem is formulated after each increment of load. This technique is known as nonlinear buckling analysis even though a linearized eigenvalue analysis is used at each stage. Linear buckling can be obtained as a special case of nonlinear buckling with only one increment.

For highly nonlinear collapse problems, full nonlinear analyses are preferred to obtain an effective and accurate solution. This technique allows the description of the equilibrium path in a space defined by the nodal variables and the loading parameter. Control techniques are available to deal with unstable problems where the load and/or the displacement value may increase or decrease as the solution progresses.

Despite the fact that all these analysis techniques have been implemented in most commercial codes, many users still model such phenomena partially through a linear buckling analysis. This technique to simulate structural collapse, has several limitations which may give inaccurate results in certain cases. These limitations are primarily due to the nature of collapse which typically involves very large displacements and rotations. The assumption that the structure behaves elastically up to the critical load may not always hold. If some part of the structure develops prebuckling plastic deformations, then the collapse or buckling analysis must include both geometrical and material nonlinearities. Recent works (Zhou et al., 2011 and Novoselac et al., 2012) compare the effects of including or not such nonlinearities in the critical load estimation.

In this study, the limit load of a circular shallow arch was investigated through linear buckling, nonlinear buckling and full nonlinear analysis. This classical problem was studied by Yaw et al. (2008) including only geometrical nonlinearity. One aim of the present work is to introduce material nonlinearity considering elastoplastic behavior.

Based on a Total Lagrangian formulation and under the assumption of small deformations, a FE program has been developed in order to model large displacement problems. The advantages of this formulation are better explored by considering the oriented body (beam) as a continuum using isoparametric bidimensional elements with nine nodes (Q9). This theoretical background has been provided by the works of Wood and Zienkiewicz (1977) and Guimarães (2006).

The easiest way to consider material nonlinearities is by means of plastic analyses. An incremental flow theory has been adopted in this work, and a von Mises material with isotropic hardening has been taken.

2 BASICS OF COLLAPSE ANALYSIS

Most commercial FE codes can model the collapse phenomena through three different techniques: linear buckling analysis, nonlinear buckling analysis and full nonlinear analysis. There are many others in the literature but these techniques are the most commonly used in commercial codes.

2.1 Linear buckling analysis

Linear buckling analysis is generally used to estimate the critical load of an ideal linear elastic structure. In this technique an eigenvalue problem is formulated to calculate the critical load that turns singular the stiffness matrix of the structure. It is assumed that the structure's configuration does not change during the process of loading. Through an eigenvalue analysis, the critical load is estimated by:

$$\left|K_0^* + \omega K_G^*\right| = 0 \tag{1}$$

Where K_0^* is the initial stiffness matrix defined as:

$$K_0^* = \int_{V_0} {B_{L0}}^T C^e B_{L0} dV \tag{2}$$

And K_G^* is the geometrical stiffness matrix defined as:

$$K_G^* = \int_{V_0} {B_{NL}}^T \sigma \; B_{NL} dV \tag{3}$$

In the above equations, B_{L0} and B_{NL} are the constant part of the linear strain-displacement matrix and the nonlinear strain-displacement matrix, respectively, C^e is the elastic matrix, σ is the matrix representation of the stress tensor, and ω is the buckling load factor. More literature details about this topic can be found in McGuire et al. (2000) and De Borst et al. (2012).

2.2 Nonlinear buckling analysis

An eigenvalue analysis can also be performed for critical load in a nonlinear problem based on the incremental stiffness matrices. This type of analysis estimates the maximum load that can be applied to a moderately nonlinear structure before instability happens or, in other words, when the structure's stiffness matrix approaches to a singular value. Collapse problems that involve material and geometrical nonlinearities must be solved incrementally. Hence, a failure to achieve converge in the iteration process or a nonpositive definite stiffness matrix determines the structural collapse. Nonlinear material properties and large displacements were considered in the nonlinear buckling analysis of the structure.

Solving the eigenvalue problem that is formulated after each increment of load, we can obtain the updated critical load estimation for that load level. The eigenvalue problem is defined as:

$$\left[K + \omega \Delta K_G\left(\Delta u, u, \Delta\sigma\right)\right]\{\phi\} = \{0\} \tag{4}$$

Where ΔK_G is known as the increment of the geometric stiffness matrix and K is tangent stiffness matrix in the beginning of the increment. The critical load P_{cr} is estimated by:

$$P_{cr} = P + \omega \Delta P \tag{5}$$

Where P is the load applied in the beginning of the increment, ΔP is the load increment and ω is the buckling load factor within the increment. Linear buckling can be considered as a special case of nonlinear buckling assuming that all behavior prior to buckling or collapse is linear.

Three types of geometric stiffness matrix were considered in the present work in order to assess the performance of different matrix formulations. In a classical work, Dupuis et al. (1970) proposed that the geometric stiffness can be assembled as:

$$K_G = K_1 + K_2 \tag{6}$$

Where K_1 is the initial displacement stiffness matrix defined as:

$$K_1 = \int_{V_0} B_{L0}{}^T C\ B_{L1} dV + \int_{V_0} B_{L1}{}^T C\ B_{L0} dV + \int_{V_0} B_{L1}{}^T C\ B_{L1} dV \tag{7}$$

And K_2 is the initial stress stiffness matrix defined as:

$$K_2 = \int_{V_0} B_{NL}{}^T \sigma\ B_{NL} dV \tag{8}$$

In the above equations, B_{L1} is the displacement dependent part of the linear strain-displacement matrix, C is the tangent stress-strain matrix, and B_{L0}, B_{NL} and σ were defined in Eq. (2) and Eq. (3), respectively. More recently, Waszczyszyn et al. (1994) suggested that the part of matrix K_1 which is quadratically dependent on the displacements may be neglected. This geometric stiffness matrix can be rewritten as:

$$K_G = K_{u1} + K_2 \tag{9}$$

Where K_{u1} is the linear part of the displacement in matrix K_1 defined as:

$$K_{u1} = \int_{V_0} B_{L0}{}^T C\ B_{L1} dV + \int_{V_0} B_{L1}{}^T C\ B_{L0} dV \tag{10}$$

Another formulation considered is the classical geometric matrix widely used in classical buckling problems. This matrix neglects the initial displacement matrix K_1 and is defined as:

$$K_G = K_2 \tag{11}$$

2.3 Full nonlinear analysis

The full nonlinear analysis is chosen for extremely nonlinear problems that show a complicated behavior in the load-deflection response. For instance, the load and/or the displacement may reduce as the solution progresses. This technique deals with large displacements and nonlinear material properties in a quasi-static fashion along the entire load-deflection path up to and possibly beyond the critical load level. Therefore, the post-buckling behavior of structures such as elastic-plastic snap-through and snap-back phenomena can be handled through this analysis.

The nonlinear equations in the jth iteration of the ith incremental step can be written as:

$$\left[K_{j-1}^{i}\right]\left\{\Delta U_{j}^{i}\right\}=\lambda_{j}^{i}\left\{\overline{P}\right\}+\left\{R_{j-1}^{i}\right\} \tag{12}$$

In the above equation $\left[K_{j-1}^{i}\right]$ is the tangent stiffness matrix, $\left\{\Delta U_{j}^{i}\right\}$ is the displacement increment vector, $\left\{\overline{P}\right\}$ is the reference load vector, $\left\{R_{j-1}^{i}\right\}$ is the unbalanced load vector and λ_{j}^{i} is the load increment factor. This factor can be determined from the constraint imposed by each iterative scheme.

Three iterative methods were implemented in the developed program: load control method, displacement control method and arch length method. More literature details about these iterative methods can be found in Yang and Kuo (1994) and Souza Neto et al. (2008).

3 GEOMETRY AND FINITE ELEMENT MODEL

The geometry and material properties of the studied circular shallow arch are shown in Fig. 1. The arch is hinged at both ends and the span length from pin to pin is 2540 mm. The FE model was done in the developed program. For analysis, continuum quadrilateral elements with 9 nodes (Q9) were used and two different FE meshes were employed for the elastic and elastoplastic case. The load was applied by a concentrated load at the top of the section.

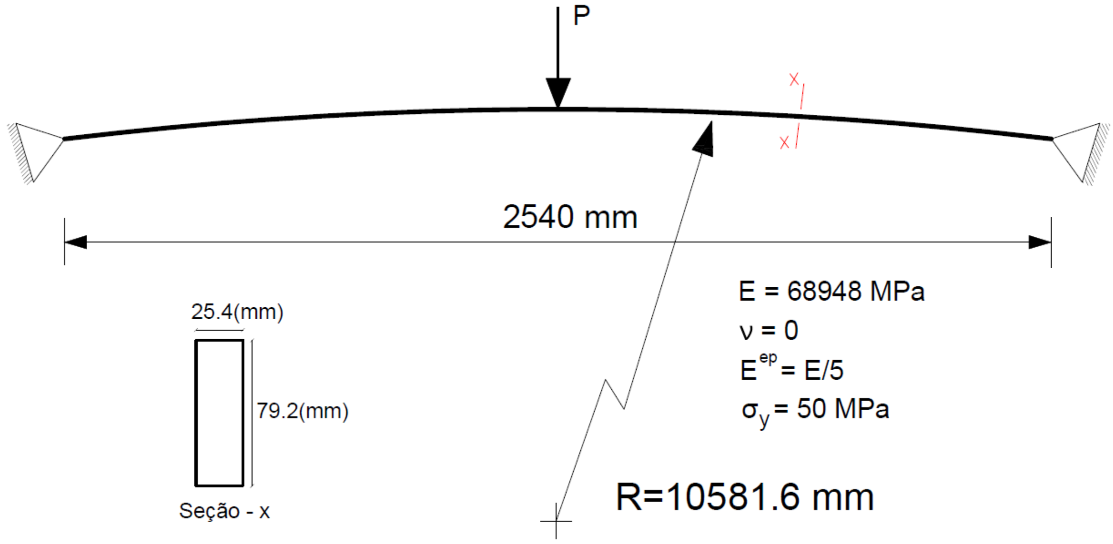

Figure 1. Initial arch configuration and material properties

For the elastic case the arch was modeled with twenty isoparametric elements Q9 in the circumferential direction as shown in Fig. 2. The numerical integration employed nine Gauss points.

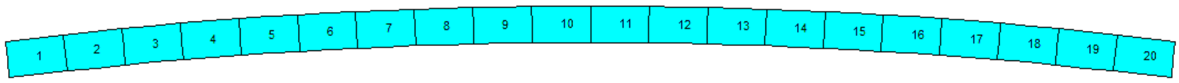

Figure 2. Finite element model for elastic case

For the elastoplastic case the arch was modeled with eighty isoparametric elements Q9, forty and two divisions in the circumferential and radial direction, respectively, as shown in Fig. 3. In this case a more refined mesh is needed in order to model the material nonlinearity with enough accuracy. The numerical integration also employed nine Gauss points.

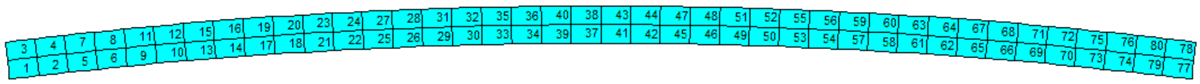

Figure 3. Finite element model for elastoplastic case

4 RESULTS

The arch's collapse analysis was performed through the three studied techniques for determination of the critical load and the collapse configuration. A linear buckling analysis was done first considering the initial stiffness matrix. Then a nonlinear buckling was done considering an updated stiffness matrix at the beginning of each incremental load. Finally, a full nonlinear analysis was carried out considering an updated stiffness matrix throughout the entire process.

In the comparison presented herein, the different formulations of the geometric stiffness matrix developed by Dupuis et al. (1970), Waszczyszyn et al. (1994) and the classical formulation were renamed as formulation I, formulation II and formulation III, respectively.

Furthermore, to compare the material behavior and their influence in the collapse analysis, linear-elastic and nonlinear elastoplastic material behavior were studied separately.

4.1 Results for the elastic case

From linear buckling analysis, a critical load value of 78.3kN was obtained. The first buckling mode related to this load value is asymmetric as shown in Fig. 4.

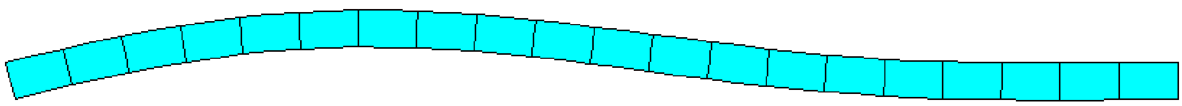

Figure 4. Linear buckling analysis - first buckling mode

For the nonlinear buckling analysis, a load value of 26kN was applied in 26 increments. In this analysis the critical load is estimated after every load increment. The obtained load values after increment 10, 15, 20, 23 and 26; are shown in Table 1, Table 2 and Table 3, for each geometric stiffness formulation, respectively.

Table 1. Buckling loads estimates with formulation I

N° of increment	P (kN)	ΔP (kN)	λ	Critical load (kN)
10	9	1	24.40	33.4
15	14	1	17.52	31.5
20	19	1	10.48	29.5
23	22	1	6.12	28.1
26	25	1	1.31	26.3

Table 2. Buckling loads estimates with formulation II

N° of increment	P (kN)	ΔP (kN)	λ	Critical load (kN)
10	9	1	21.30	30.3
15	14	1	13.80	27.8
20	19	1	7.10	26.1
23	22	1	3.58	25.6
26	25	1	0.54	25.5

Table 3. Buckling loads estimates with formulation III

N° of increment	P (kN)	ΔP (kN)	λ	Critical load (kN)
10	9	1	58.20	67.2
15	14	1	46.31	60.3
20	19	1	32.89	51.9
23	22	1	20.97	43.0
26	25	1	4.08	29.1

From the nonlinear buckling analysis results, it is observed that the critical loads tend to converge at load increment 26. The obtained first buckling modes corresponding to formulation I and II were all symmetric after each load increment. Similarly to the results linear buckling analysis, the buckling modes of formulation III after load increments 10, 15 and 20 were asymmetric. Contrarily, the buckling modes obtained after load increments 23 and 26 were symmetric in the same way of formulations I and II. The buckling mode after load increment 26 is shown in Fig. 5.

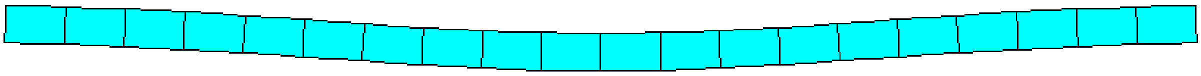

Figure 5. Nonlinear buckling analysis - first buckling mode after load increment 26

Finally, from the full nonlinear analysis, a critical load value of 26.1kN was obtained. The load-displacement curve (equilibrium path) corresponding to elastic FE model is shown in Fig.6 via a history plot of the reference node (i.e. the node in which the load is applied). The deformed configuration at the critical load is shown in Fig.7.

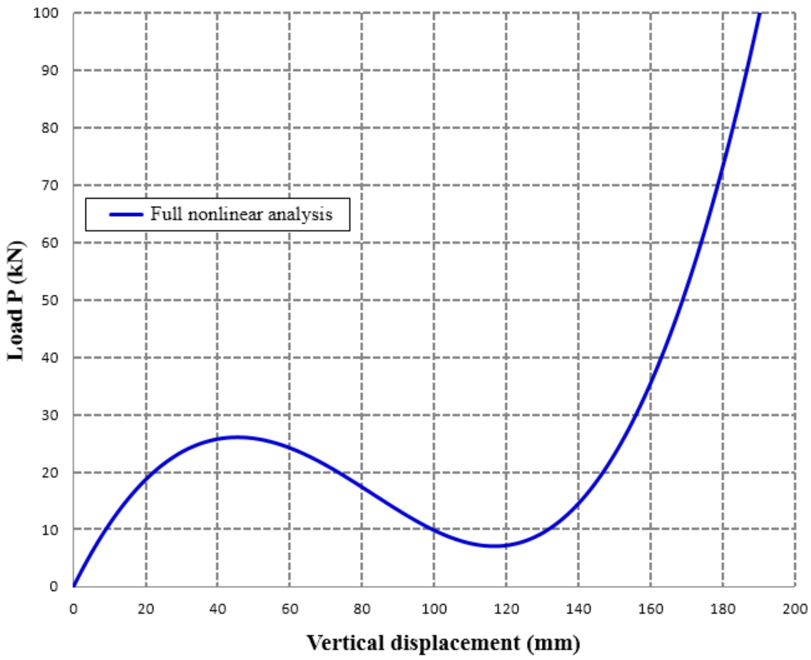

Figure 6. Full nonlinear analysis - load-displacement curve for the elastic case

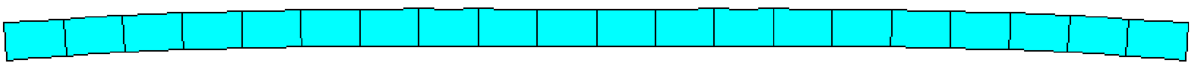

Figure 7. Full nonlinear analysis - deformed configuration at critical load

The differences between the critical loads obtained with each technique and applied formulation for the elastic case are summarized and plotted in Fig.8. It can be observed that when numbers of steps is increased the critical loads of nonlinear buckling analysis converges to the full nonlinear solution. On the other hand, the unique solution provided by the linear buckling analysis differs considerably from the accurate nonlinear result. Additionally, formulations I and II show faster convergence and better accuracy than formulation III.

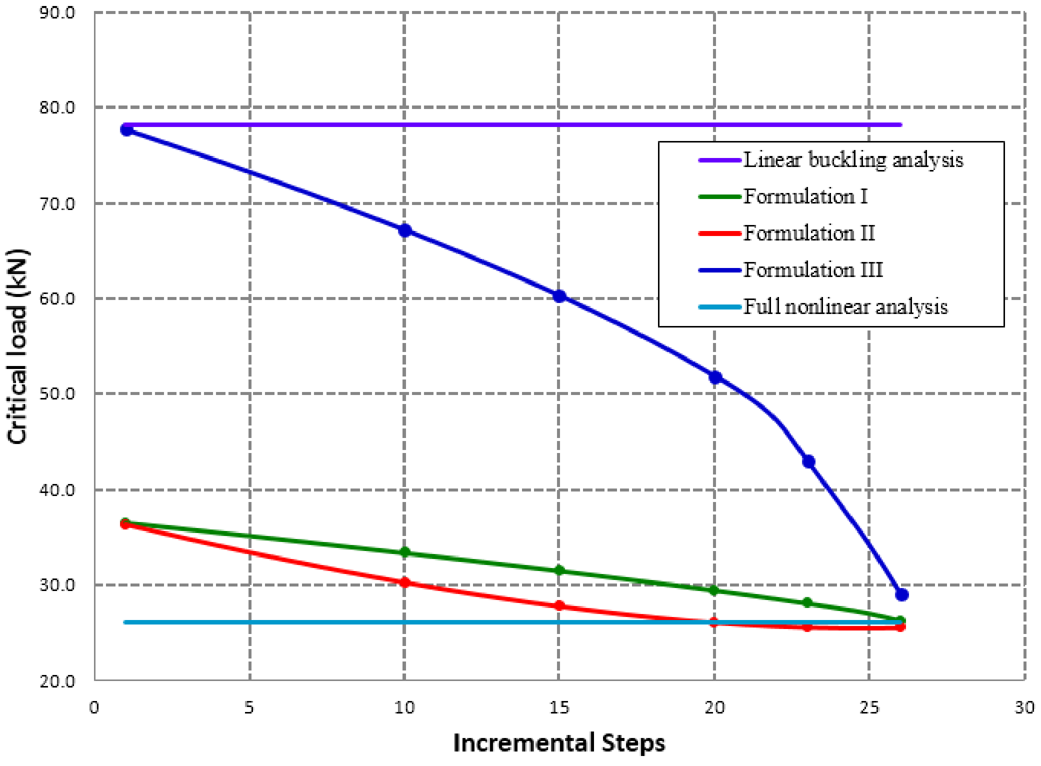

Figure 8. Obtained critical load values from different techniques and formulations

The stress distribution for the elastic case are shown in Fig.9, by means of the equivalent von Mises stresses obtained for linear and full nonlinear FEA. To obtain the stresses distribution in the arch, a load with the same value as the obtained critical load from full nonlinear analysis was applied in both FEA.

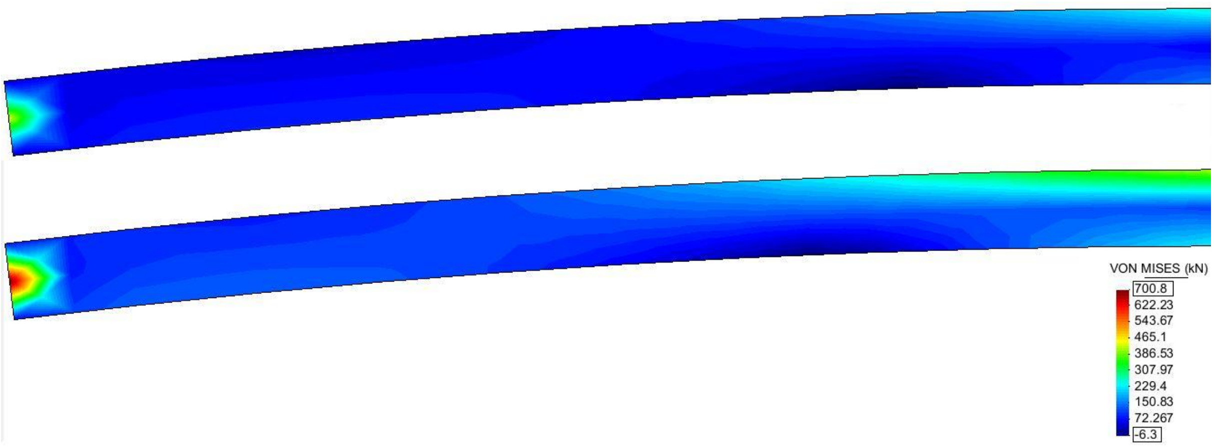

Figure 9. Equivalent von Mises stresses for linear and nonlinear analysis, respectively

4.2 Results for the elastoplastic case

A critical load value of 78.6kN was obtained from linear buckling analysis. The first buckling mode, related to this load value, is asymmetric as shown in Fig. 10. As expected, the results are very similar to obtained results with the previous mesh.

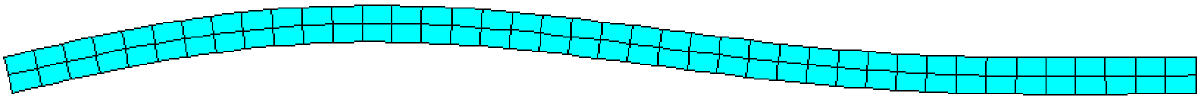

Figure 10. Linear buckling analysis - first buckling mode

For the nonlinear buckling analysis, a load value of 11.5kN was applied in 23 increments. In this analysis the critical load is estimated after every load increment. The obtained load values after increment 10, 15, 18, 21 and 23 are shown in Table 4, Table 5 and Table 6, for each of the three geometric stiffness formulation, respectively.

Table 4. Buckling loads estimates with formulation I

N° of increment	P (kN)	ΔP (kN)	λ	Critical load (kN)
10	4.5	0.5	53.96	31.5
15	7	0.5	32.19	23.1
18	8.5	0.5	20.12	18.6
21	10	0.5	10.56	15.3
23	11	0.5	2.56	12.3

Table 5. Buckling loads estimates with formulation II

N° of increment	P (kN)	ΔP (kN)	λ	Critical load (kN)
10	4.5	0.5	50.40	29.7
15	7	0.5	28.14	21.1
18	8.5	0.5	16.33	16.7
21	10	0.5	7.53	13.8
23	11	0.5	1.16	11.6

Table 6. Buckling loads estimates with formulation III

N° of increment	P (kN)	ΔP (kN)	λ	Critical load (kN)
10	4.5	0.5	139.14	74.1
15	7	0.5	111.82	62.9
18	8.5	0.5	90.22	53.6
21	10	0.5	53.51	36.8
23	11	0.5	10.09	16.0

From the nonlinear buckling analysis results, it is observed that the critical loads tend to converge at load increment 23. The obtained first buckling modes in formulation I and II were all symmetric after each load increment. On the other hand, the obtained modes in formulation III after load increment 10, 15 and 18 were asymmetric as the previous linear eigenvalue buckling analysis, while buckling modes after load increment 21 and 23 were symmetric as the obtained modes in formulation I and II. The buckling mode after load increment 23 is shown in Fig. 11.

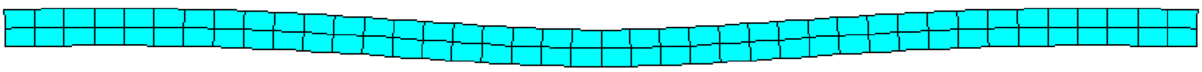

Figure 11. Nonlinear buckling analysis - first buckling mode after load increment 23

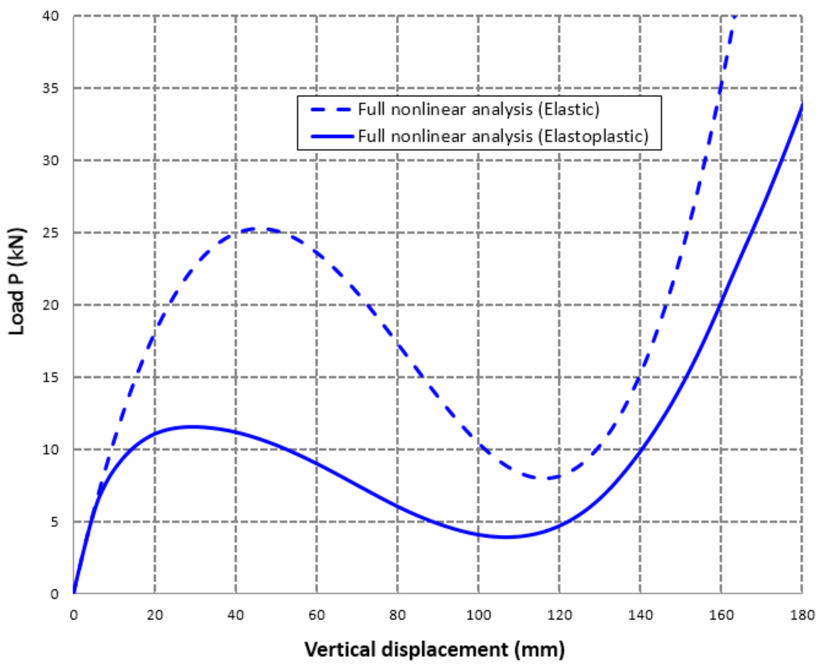

Figure 12. Full nonlinear analysis - load-displacement curve for the elastoplastic case

Finally, from the full nonlinear analysis, a critical load value of 11.5kN was obtained. The load-displacement curve (equilibrium path) for the elastoplastic FE model is shown in Fig.12 via a history plot of the reference node (i.e. the node in which the load is applied). These results show that critical load is significantly smaller than the obtained in elastic case. The deformed configuration at the critical load is shown in Fig.13.

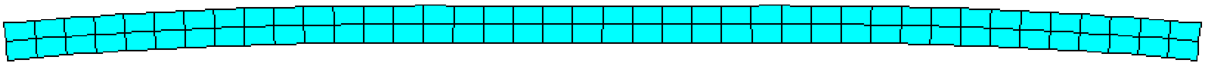

Figure 13. Full nonlinear analysis - deformed configuration at critical load

To show the differences between each technique and applied formulation in the elastoplastic case, the estimated critical loads are summarized and plotted in Fig.14. From these results, it is observed that the nonlinear buckling load converges at final increments to the full nonlinear load, whereas the linear buckling load differs considerably from both loads. In this case formulation I and II show fast convergence and better accuracy than formulation III, as in the previous elastic case.

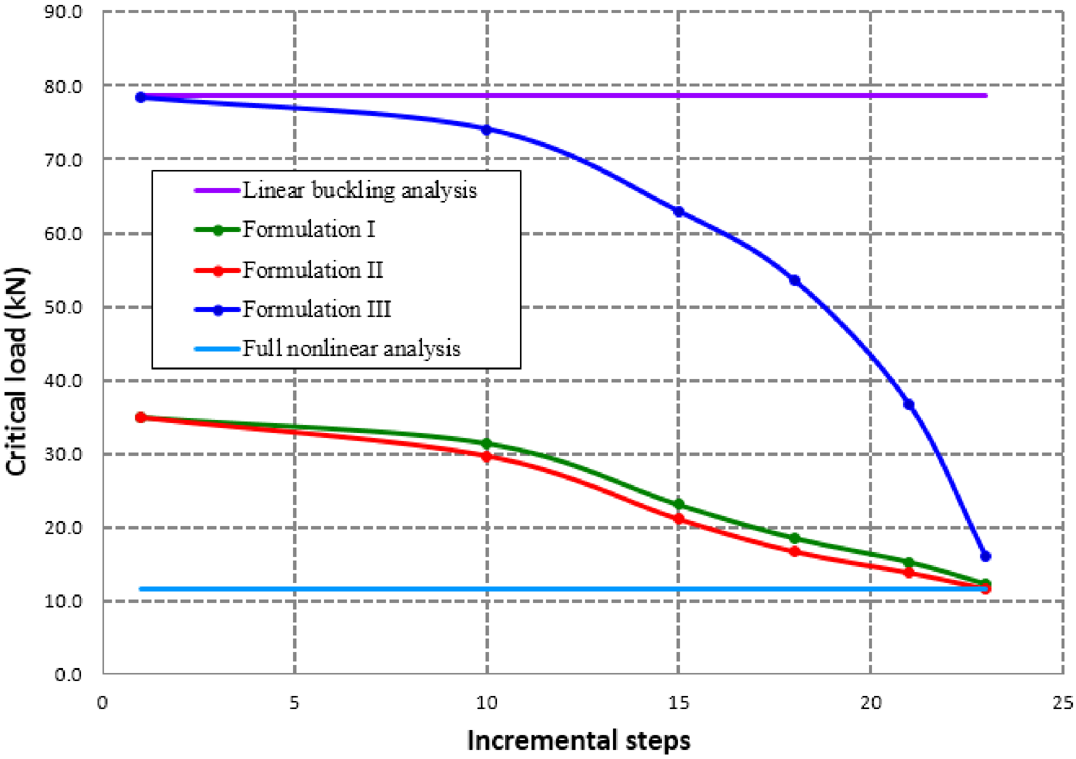

Figure 14. Obtained critical load values from different techniques and formulations

To show the stress distribution for this elastoplastic case, equivalent von Mises stresses were obtained for the linear and full nonlinear FEA. These stresses are pictured in Fig.15. To obtain stresses developed in the arch, a load with the same value as the obtained critical load from full nonlinear analysis was applied in both FEA.

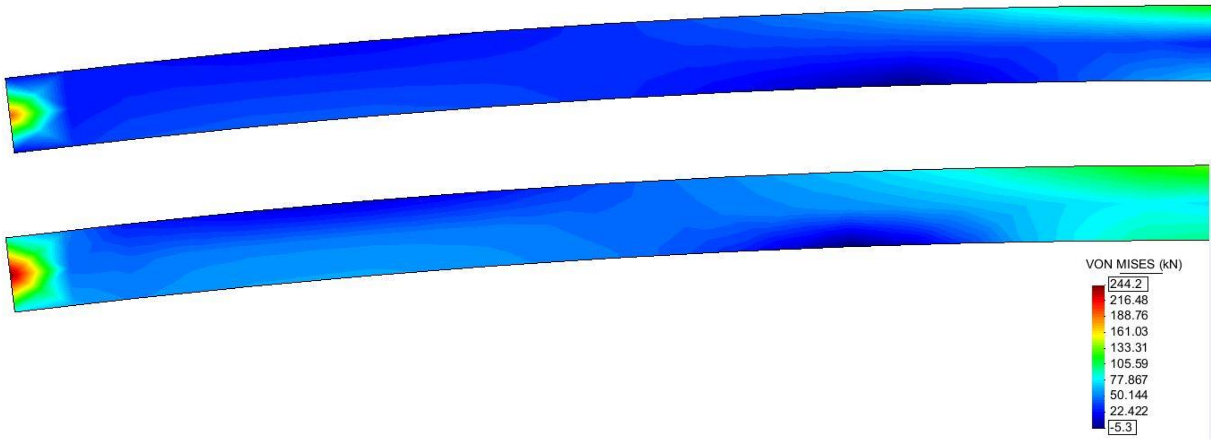

Figure 15. Equivalent von Mises stresses for linear and nonlinear analysis, respectively

5 CONCLUSIONS

The calculated critical loads and buckling modes from the nonlinear incremental buckling analysis and full nonlinear analysis are close to each other.

Inaccurate critical loads and buckling modes were obtained when employing the linear buckling analysis. This is mainly due to the assumption that pre-buckling displacements are sufficiently small so that the shape of the stress distribution remains unchanged and only the stress levels change with a factor, which is clearly not the case. It is also shown in the calculated equivalent von Mises stresses that an internal redistribution of stresses happens and cannot be disregarded.

In the example presented in this paper, taking the effect of including the stresses only and neglecting the effect of displacements in formulation of the geometric stiffness matrix led to a slower convergence than taking the effect of these displacements in the nonlinear incremental buckling analysis.

The loss of stiffness appreciated in the elastic and the elastoplastic cases, due to geometric and material nonlinearities, causes a significant reduction of the critical load compared to the linear model. Therefore, the critical load predicted by the linear buckling analysis is usually overestimated.

The results obtained in the elastoplastic cases show that when the deformable elements of the compressed arch enter into the elasto-plastic regime, the corresponding loss of stiffness usually causes a considerable reduction of the loading capacity of the structure, since after yielding an increase in the deformation causes a decrease of the load.

Isoparametric bidimensional elements permit to take advantage of the Total Lagrangian approach resulting in an uncomplicated formulation and unrestricted magnitude of displacements and rotations, characteristic of geometric nonlinear problems.

REFERENCES

De Borst, R., Crisfield, M. A., Remmers, J. J. C., & Verhoosel, C. V., 2012. *Nonlinear Finite Element Analysis of Solids and Structures*, 2nd ed., John Wiley & Sons Ltd.

Dupuis, G. A., Pfaffinger, D. D., & Marcal, P. V., 1970. Effective Use of the Incremental Stiffness Matrices in Nonlinear Geometric Analysis. *International Union of Theoretical and Applied Mechanics*, Liège, Belgium, Technical report.

Guimarães, J., 2006. *Buckling of Viscoelastic Structures*. PhD thesis, Pontifical Catholic University of Rio de Janeiro/Brazil.

McGuire, W., Gallagher, R. H., & Ziemian, R. D., 2000. *Matrix Structural Analysis*, 2nd ed., John Wiley & Sons Ltd.

Souza Neto, E. A., Períc, D., & Owen, D., 2008. *Computational Methods for Plasticity: Theory and Applications*, 1st ed., John Wiley & Sons Ltd.

Novoselac, S., Ergić, T., & Baličević, P., 2012. Linear and Nonlinear Buckling and Post Buckling Analysis of a Bar with the Influence of Imperfections. Technical Report, vol. 19, n. 3, pp. 695-701.

Waszczyszyn, Z., Cichon, C., & Radwanska, M., 1994. *Stability of Structures by Finite Element Methods*, 1st ed., Elsevier Science B. V.

Wood, R. D., & Zienkiewicz, O. C., 1977. Geometrically nonlinear finite element analysis of beams, frames, arches and axisymmetric shells. *Computers & Structures*, vol. 7, pp. 725-735.

Yang, Y. B., & Kuo, S. R., 1994. *Theory and Analysis of Nonlinear Framed Structures*, 1st ed., Prentice Hall.

Yaw, L. L., Sukumar, N., & Kunnath, S. K., 2008. Meshfree co-rotational formulation for two-dimensional continua. *International Journal for Numerical Methods in Engineering*, vol. 79, n. 8, pp. 979-1003.

Zhou, Z., Nishida, A., & Kuwamura, H., 2011. Applicability of Finite Element Method to Collapse Analysis of Steel Connection under Compression. *Journal of Nuclear Science and Technology*, vol. 2, pp. 481-485.